Novel Gurmarin-like Peptides from *Gymnema sylvestre* and their Interactions with the Sweet Taste Receptor T1R2/T1R3

Halim Maaroufi

Institut de biologie intégrative et des systèmes (IBIS), Université Laval, Quebec City, Quebec, Canada. halim.maaroufi@ibis.ulaval.ca

Abstract

Gymnema sylvestre (GS) is a traditional medicinal plant known for its hypoglycemic and hypolipidemic effects. Gurmarin (hereafter Gur-1) is the only known peptide in GS. Gur-1 functions as a sweet taste suppressor in rodents but weakly in humans. Here, eight gurmarin-like peptides (Gur-2 to Gur-9) and their isoforms are reported in the GS transcriptome. The molecular mechanism of sweet taste suppression by Gur-1 is still largely unknown. Therefore, the complete architecture of human and mouse sweet taste receptor (STR) T1R2/T1R3 and its interaction with Gur-1 to Gur-9 were predicted by AlphaFold-Multimer (AF-M). Only Gur-1 and Gur-2 interact with T1R2 and T1R3 monomers and the T1R2/T1R3 heterodimer. AF-M predicted that Gur-1 binds to the intracellular domain (ICD) of the T1R2 monomer and to two binding sites in the cysteine rich domain (CRD) of the T1R3 monomer. In the T1R2/T1R3 heterodimer, Gur-1 binds to an additional site on the T1R2 subunit in addition to the ICD. The novel Gur-2 binds to two sites on the T1R2 monomer and one site on the T1R3 monomer, and as Gur-1 to two binding sites on the T1R2 subunit of the T1R2/T1R3 heterodimer. Furthermore, AF-M predicted that the Gα-gustducin (a role in sweet taste transduction) interacts as Gur-1 with the ICD of the T1R2 subunit in the T1R2/T1R3 heterodimer, suggesting that Gur-1 may compete with Gα-gustducin in the cell. These results highlight an unexpected diversity of gurmarin-like peptides in GS and provide the complete predicted architecture of the human and mouse sweet taste receptor with the putative binding sites of Gur-1, Gur-2 and Gα-gustducin.

Key words: AlphaFold-Multimer, knottin, Gα-gustducin, signal transduction, sweet taste suppression, competition

Introduction

Gurmarin (in reference to "Gurmar" that is mean "sugar destroyer" in Hindi) is the only disulfide-rich peptide of 35 amino acids purified from the leaves of the Indian plant *Gymnema sylvestre* (Imoto et al., 1991; Kamei et al., 1992). Gurmarin (hereafter Gur-1) contains three disulfide bridges forming a cystine knot fold (knottin fold) that confers high resistance to proteolytic, thermal, and chemical degradation (Pallaghy et al., 1994). Gur-1 suppresses the sweet taste responses to sucrose, glucose, glycine, and saccharin in rats (Imoto et al., 1991; Yoshie et al., 1994; Miyasaka and Imoto, 1995) and mice (Ninomiya and Imoto, 1995). However, Gur-1 showed no or only a very weak sweet taste effect in humans (Imoto et al., 1991). To suppress the sweet taste response, Gur-1 is thought to interact with T1R2/T1R3 in rodents (Shigemura et al., 2008; Ohkuri et al., 2009; Yasumatsu et al., 2009). The T1R2/T1R3 heterodimer, which belongs to class C G-protein-coupled receptor (GPCR), also known as seven-transmembrane (7TM) receptors, is a membrane sweet taste receptor (STR) in eukaryotes (Nelson et al., 2001). STR is expressed in taste buds. T1R2 and T1R3 monomer are also expressed in the gastrointestinal tract (Bezençon et al., 2007), pancreas (Nakagawa et al., 2009; Kyriazis et al., 2012), brain (Ren et al., 2009; Kohno et al., 2016), and testis (Mosinger et al., 2013). T1R2/T1R3 consists of an N-terminal extracellular ligand-binding (LB) domain (also called Venus flytrap module (VFTM)), a cysteine-rich domain (CRD), the seven-helical transmembrane domain (TMD), and a C-terminal intracellular domain (ICD). In humans and rodents, the T1R2/T1R3 receptor recognizes sweet substances such as sugar. Interestingly, a systematic review and meta-analysis have shown that *G. sylvestre* supplementation has a beneficial effect on glycemic and lipid control in patients with type-2 diabetes mellitus (Devangan et al., 2021). Unfortunately, Gur-1 has a very weak sweet taste effect on humans. Therefore, the search for other gurmarin-like peptide(s) with sweet taste effect in humans will be important for the development of antidiabetic molecules. In this study, the search for the Gur-1 homologs in the *G. sylvestre* transcriptome revealed a rich arsenal of gurmarin-like peptides. Furthermore, the predicted architecture of the human and mouse sweet taste receptor (STR) T1R2/T1R3 and their interaction with Gur-1 and Gur-2 suggest that the sweet taste suppression in rodents by Gur-1 is probably due to its interaction with T1R3 that inhibits the formation

of the T1R2/T1R3 heterodimer. Gurmarin-like peptides found in GS could be an interesting drug scaffold for the development of antidiabetic molecules.

Materials and methods

Search for Gur-1-like peptides in *G. sylvestre*

TblastN algorithm (http://www.ncbi.nlm.nih.gov/blast) with Gur-1 (UniProt ID: P25810) as query is used to search in *de novo* transcriptome (RNA-seq) sequences of leaf, flower and developing fruits of *G. sylvestre* genotype DGS-22 deposited in NCBI Short Read Archive (SRA) (SRA accession ID: SRR5965323, SRR5965320, SRR5965321) (Kalariya et al., 2019). And also, in leaves prior to flowering of *G. sylvestre* genotype DGS-3 (SRA accession ID: SRR5965322) (Kalariya et al., 2018). TblastN is also used to search for Gur-1-like peptides in the transcriptome of plant samples (SRA accession ID: SRR7876667) and leaf tissues (SRA accession ID: SRR3664033) of *G. sylvestre* (Ayachit et al., 2019).

Chemical properties of gurmarin-like peptides

The chemical structures and properties of gurmarin-like peptides were investigated *in silico* using PepDraw (http://www.tulane.edu/~biochem/WW/PepDraw/index.html) as described in Maaroufi and collaborators (Maaroufi et al., 2021).

Phylogeny

Multiple sequences alignment are conducted by Mafft (Katoh and Toh, 2008) and phylogenetic tree is constructed by PhyML (Guindon et al., 2010).

Residue numbering

The amino acid residues in Gur-1, Gur-2, mouse and human T1R2 and T1R3 are numbered without signal peptide.

Structure prediction with AlphaFold2 and AlphaFold-Multimer

The AlphaFold2 (AF2) and AlphaFold-Multimer (AF-M) source code was installed locally on a Linux workstation with NVIDIA Quadro RTX6000 GPU.

The structure of Gur-1 has already been determined (PDB ID: 5OLL), while Gur-2 to Gur-9 peptides were predicted using AF2, while AF-M was used to predict the likely complex formation with different combinations of Gur-1 to Gur-9 peptides, T1R2 and T1R3 from mouse (UniProt ID: Q925I4 and Q925D8) and human (UniProt ID: Q8TE23 and Q7RTX0) (Jumper et al., 2021; Evans et al., 2022).

AF-M is also used to study the interactions of Gur-1, Gur-2 with mouse T1R2, T1R3 and the Gα-gustducin (GNAT3) (UniProt ID: Q3V3I2).

To test the accuracy of AF-M, the brazzein peptide (UniProt ID: P56552) that has been studied experimentally for its interactions with T1R2 and T1R3 has been used as in put in AF-M with T1R2 and T1R3.

AF2 and AF-M generate five ranked models. Each of the five predicted structure was examined.

The structure figures were generated with PyMOL (http://www.pymol.org).

Molecular dynamics simulations

In order to evaluate conformational changes of Gur-1 (PDB ID: 5OLL) and Gur-2 (3D predicted by AF2), molecular dynamics (MD) simulations were performed in GROMACS (2021.4) using the OPLS-AA/L all-atom force field (Kaminski et al., 2001) as described in (Maaroufi et al., 2021), except that Gur-1 and Gur-2 MD simulations were performed for 100 ns and in triplicate.

Structural similarity search

DALI (http://ekhidna2.biocenter.helsinki.fi/dali/), Foldseek (https://search.foldseek.com/search) and the PDB website software (https://www.rcsb.org/search/advanced/structure) were used to search for structural similarities of Gur-1 to Gur-9, T1R2 and T1R3 in the PDB and AlphaFold databases (van Kempen et al., 2023).

Membrane topology prediction

Membrane T1R2/T1R3 topology prediction was conducted by MembraneFold (https://ku.biolib.com/MembraneFold/) (Gutierrez et al., 2022).

Binding affinity

The PRODIGY web server (https://wenmr.science.uu.nl/prodigy/) was used to calculate the binding free energies (ΔG) of interacting protein-protein and peptide-protein complexes (Xue et al., 2016).

Amino acids interactions in protein-protein complex

Protein Interactions Calculator (PIC) is used to determine different bonds between amino acids residues (http://pic.mbu.iisc.ernet.in/).

Results and discussion

G. sylvestre transcriptome is rich in gurmarin-like peptides

Gurmarin (hereafter Gur-1) is the only peptide extracted from the leaves of *Gymnema sylvestre* (Imoto et al., 1991; Kamei et al., 1992). In the aim to find homologs of Gur-1 (UniProt ID: P25810), a TblastN was performed using the transcriptome (RNA-seq) sequences of leaves, leaves prior to flowering, flowers and developing fruits of *G. sylvestre* deposited in the NCBI Short Read Archive (SRA) (Kalariya et al., 2018, 2019; Ayachit et al., 2019). From this search, 57 gurmarin-like peptides were found. Multiple sequence alignment (MSA) of these peptides revealed nine groups, named Gur-I to Gur-IX (Fig. 1). Gur-I group is rich in isoforms of Gur-1. Interestingly, Trp29, whose mutation to alanine completely abolishes the sweet-suppressing properties of Gur-1, is conserved in isoforms of Gur-1 and Gur-2 (Sigoillot et al., 2018).

It has been found that Gur-1 has a very weak suppressive sweet taste effect in humans (Imoto et al., 1991; Miyasaka and Imoto, 1995). Therefore, this arsenal of isoforms may have a more potent sweet taste inhibitory effect in humans. It is noteworthy that some of

these isoforms have mutations in Cys10 or Cys17 and Cys10/Cys17. Gur-1 has three disulfide bridges (Cys3-Cys18, Cys10-Cys17 and Cys23-Cys33). Interestingly, it has been shown that mutagenesis of these six cysteines alters the function of Gur-1. Indeed, mutant Gur-1 analogs with only two native disulfide bonds suppressed the response to sucrose, but not those to glucose, fructose, saccharin, or glycine in rats (Ota et al., 1998b).

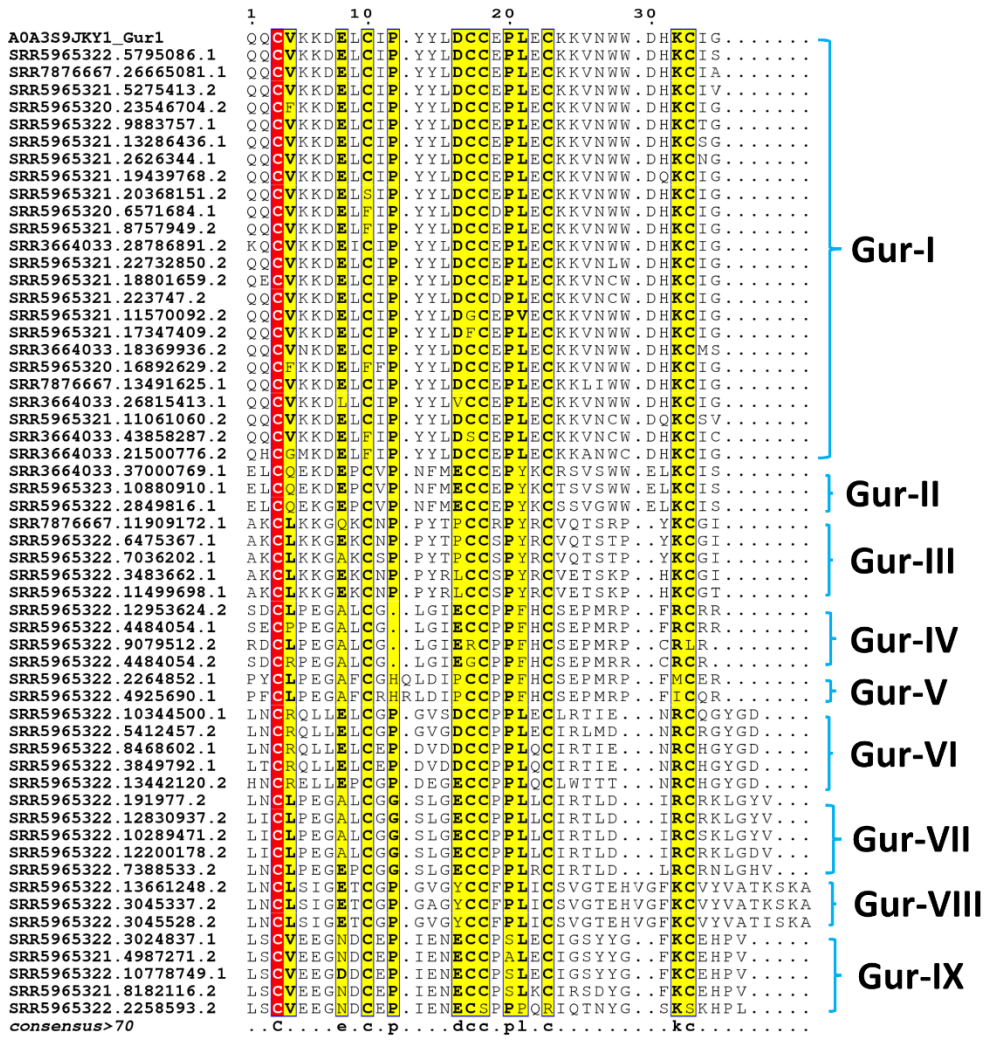

Fig. 1. Multiple sequence alignment of *G. sylvestre* gurmarin-like peptides. The sequences are divided to nine groups, named Gur-I to Gur-IX. Gur-I group that contains Gur-1 and its isoforms is the large group. Trp28 and Trp29 that are important for the suppressive sweet taste effect are conserved in groups Gur-I and Gur-II.

For the continuation of this study, one representative sequence from each group of gurmarin-like peptides was selected and named Gur-1 (from group I) to Gur-9 (from group IX) (Fig. 2). The analysis of Gur-1 to Gur-9 showed that they have different physicochemical properties (Table 1). Gur-2 is more similar to Gur-1 (51% of identity and 77% of similarity in amino acid residues). Like Gur-1, Gur-2 has a hydrophobic and hydrophilic cluster on the surface of the molecule (Ota et al., 1998a).

For Gur-3 to Gur-9, BlastP (expect threshold of 0.05) against the NCBI database showed no matches, indicating that they are novel knottin peptides.

```
                                  1         10          20          30
Gur-1_P25810                      QQCVKKDELCIPYYL.DCCEPLECKKVNW.WDHKCIG.......
Gur-2_SRR3664033.37000769.1       ELCQEKDEPCVPNFM.ECCEPYKCRSVSW.WELKCIS.......
Gur-3_SRR7876667.11909172.1       AKCLKKGQKCNPPYT.PCCRPYRCVQTS..RPYKCGI.......
Gur-4_SRR5965322.12953624.2       SDCLPEGALCG..LGIECCPPFHCSEPM..RPFRCRR.......
Gur-5_SRR5965322.2264852.1        PYCLPEGAFCGHQLDIPCCPPFHCSEPM..RPFMCER.......
Gur-6_SRR5965322.10344500.1       LNCRQLLELCGPGVS.DCCPPLECLRTI...ENRCQGYGD....
Gur-7_SRR5965322.12830937.2       LICLPEGALCGGSLG.ECCPPLLCIRTL...DIRCRKLGYV...
Gur-8_SRR5965322.13661248.2       LNCLSIGETCGPGVG.YCCFPLICSVGTEHVGFKCVYVATKSKA
Gur-9_SRR5965322.3024837.1        LSCVEEGNDCEPIEN.ECCPSLECIGSY..YGFKCEHPV.....
consensus>70                      ..C......C.......CC.p..C..........C.........
```

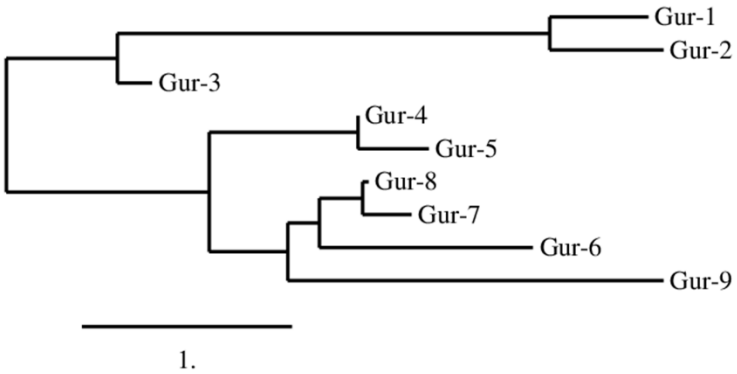

Fig. 2. Multiple sequence alignment and clustering of Gur-1 to Gur-9 peptides. Six conserved cysteines that are predicted to form a knottin three disulfide bonds.

Table 1. Physico-chemical characteristics of Gur-1 and gurmarin-like peptides

	Mature peptide	Length	Net charge	pI	Hydrophobicity (Kcal/mol)
Gur-1	QQCVKKDELCIPYYLDCCEPLECKKVNWWDHKCIG	35	-1	5.44*	+37.23
Gur-2	ELCQEKDEPCVPNFMECCEPYKCRSVSWWELKCIS	35	-3	4.18	+35.02
Gur-3	AKCLKKGQKCNPPYTPCCRPYRCVQTSRPYKCGI	34	+8	9.76	+29.10
Gur-4	SDCLPEGALCGLGIECCPPFHCSEPMRPFRCRR	33	0	6.76	+28.49
Gur-5	PYCLPEGAFCGHQLDIPCCPPFHCSEPMRPFMCER	35	-1	5.20	+24.80
Gur-6	LNCRQLLELCGPGVSDCCPPLECLRTIENRCQGYGD	36	-2	4.19	+30.56
Gur-7	LICLPEGALCGGSLGECCPPLLCIRTLDIRCRKLGYV	37	+1	7.60	+19.76
Gur-8	LNCLSIGETCGPGVGYCCFPLICSVGTEHVGFKCVYVATKSKA	43	+1	7.61	+23.80
Gur-9	LSCVEEGNDCEPIENECCPSLECIGSYYGFKCEHPV	36	-7	3.59	+40.12

*The experimental pI is 4.5 (Imoto et al. 1991).
http://wimleylab.tulane.edu/PepDraw/index.html

Prediction of the structure of the gurmarin-like peptides

The structure of Gur-1 is known (PDB ID: 5OLL). AlphaFold 2 (AF2) is used to predict the structures of Gur-2 to Gur-9. AF2 produces five ranked models. Each of the five predicted structures was examined. AF2 predicted all gurmarin-like peptides except the structure of Gur-6. Of note, the three disulfide bridges in the Gur-5 model are different from those in Gur-1. Therefore, ESMFold that uses only the amino acid sequence to predict the structure is used to predict the structure of Gur-5 and Gur-6 (Lin et al., 2023). The results of the structure alignments of Gur-1 to Gur-9 using DALI (Holm, 2020) are shown in Table 1S. The structural similarity dendrogram of Gur-1 to Gur-9 shows that the structures of Gur-2 to Gur-5 are close to Gur-1 (known function), whereas Gur-6/Gur-8 and Gur-7/Gur-9 are distant from Gur-1 (Fig. 1S).

Prediction of the structure of the T1R2/T1R3 complex

There is no experimental structure of the monomers or the complete sweet taste receptor T1R2/T1R3. Only the extracellular ligand-binding domains (LBDs or VFTM) of the medaka fish T1R2/T1R3 heterodimer have been determined (PDB ID: 5X2M). Therefore, AF2 and AlphaFold-Multimer (AF-M) were used to predict the structure of the monomers and the T1R2/T1R3 heterodimer of human and mouse, respectively. AF-M generates five ranked models. Each of the five predicted structures was examined. Recently, at CASP15, the accuracy of AF-M has been demonstrated in modeling the quaternary structure of proteins was demonstrated in comparison to bioinformatics methods used prior to AF software (Ozden et al., 2023).

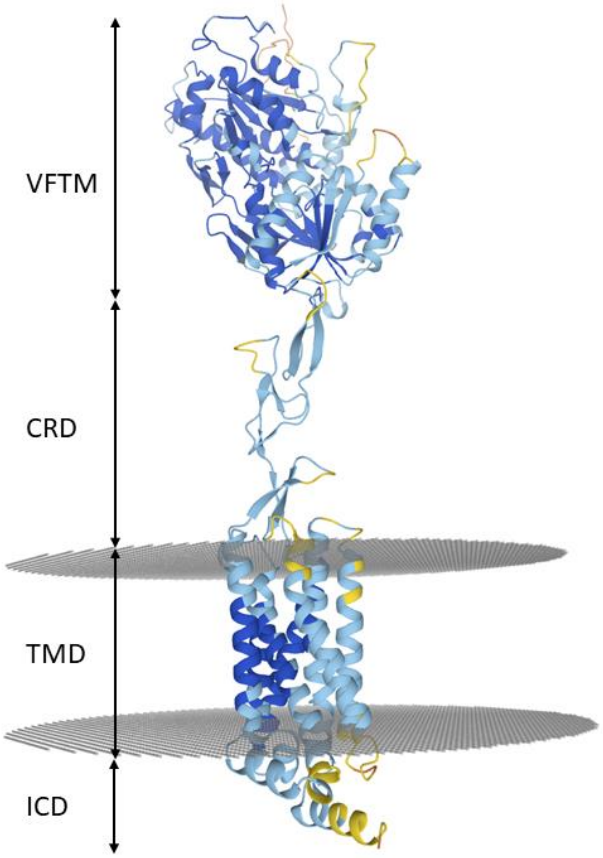

Fig. 3. The predicted structure of the mouse T1R2 (mT1R2) by AlphaFold 2 (AF2). Membrane mT1R2 topology is predicted by MembraneFold software. mT1R2 is formed with an N-terminal Venus flytrap module (VFTM), a cysteine rich domain (CRD), a heptahelical transmembrane domain (TMD) and an intracellular domain (ICD). The accuracy of the predicted model is visualized by different colors (pLDDT ≥ 90, 90>pLDDT≥70, 70>pLDDT≥50, 50>pLDDT).

The human T1R2/T1R3 (hT1R2/T1R3) complex generated by AF-M contains an ionic bond between hT1R2 Arg217 and hT1R3 Glu217. Indeed, by mutating of hT1R2 Arg217A, Cui and coworkers have suggested that Arg217 is involved in the hT1R2-T1R3 interaction (Cui et al., 2006). Furtheremore, the predicted binding affinity of hT1R2 and hT1R3 in heterodimer is -21.0 kcal/mol, and -23.1 kcal/mol for mT1R2 and mT1R3.

The structure similarity search (https://www.rcsb.org/search/advanced/structure) revealed that the predicted structure of human and mouse T1R2 and T1R3 monomers are

structurally similar to the human calcium-sensing receptor (CaSR) (PDB ID: 7M3G_A) and human metabotropic glutamate receptor 2 (mGlu2) (PDB ID: 8JD3_A). Like T1R2 and T1R3, CaSR and mGlu2 are a class C G protein-coupled receptors (GPCRs). Pairwise structure alignment (https://www.rcsb.org/alignment) using the jFATCAT (flexible) option, aligned T1R2 and T1R3 monomers to CaSR and mGlu2 with an RMSD of 3.1-3.21 Å at 723-765 amino acid residues, and 2.71-3.76 Å at 700-740 amino acid residues, respectively. Whereas, T1R2 and T1R3 are aligned to the LBDs of the medaka fish T1R2/T1R3 heterodimer (PDB ID: 5X2M) with an RMSD of 1.89-2.18 Å on 427-440 amino acid residues.

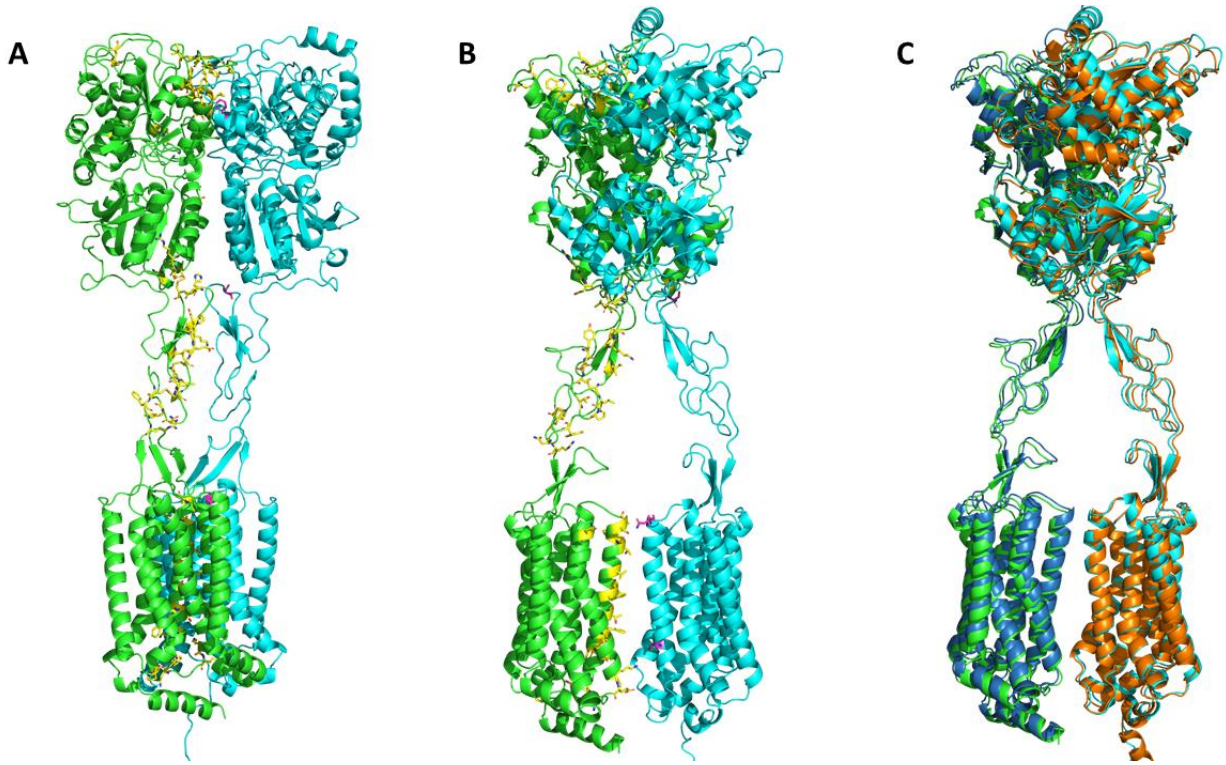

Fig. 4. Structures of human T1R2/T1R3 (hT1R2/T1R3) and mouse T1R2/T1R3 (mT1R2/T1R3) heterodimer predicted by AlphaFold-Multimer (AF-M). **A** and **B**, hT1R2/T1R3 (green/cyan) with amino acids (yellow) of hT1R2 implicated in the interactions with hT1R3 according to (Park et al., 2019). **C**, superposition of hT1R2/T1R3 (green/cyan) and mT1R2/T1R3 (blue/orange). The structure of mT1R2/T1R3 aligns on hT1R2/T1R3 with 1.445 Å.

Prediction of interactions between gurmarin-like peptides and T1R2, T1R3

In situ studies suggest that Gur-1 sensitivity is related to the coupling of T1R2/T1R3 to Gα-gustducin (Shigemura et al., 2008; Ohkuri et al., 2009; Yasumatsu et al., 2009). In addition, the recombinant Gur-1 has been shown to be responsible for the complete blockade of saccharin responses in rat T1R2/T1R3-expressing cells (Sigoillot et al., 2012). Therefore, to try to know the molecular mechanism of Gur-1 sweet taste suppression, interactions of mouse and human T1R2 and T1R3 with Gur-1 to Gur-9 were predicted by AF-M. Indeed, it has been demonstrated that AF-M (Evans et al., 2022) has been shown to be capable of predicting peptide-protein complex with high accuracy (Chang and Perez, 2023; Teufel et al., 2023). Before using AF-M to predict the interactions of Gur-1 to Gur-9 interactions with T1R2 and T1R3, the published experimental results of the interaction of Brazzein (Brz), a peptide of 54 amino acids, member of sweet-tasting peptides, with hT1R2 and hT1R3 were used to test the accuracy of the AF-M software for predicting the peptide-protein interactions. Using the hT1R2, hT1R3 and Brz amino acid sequences as input to AF-M showed only the formation of the hT1R2/hT1R3 complex was observed. The use of the hT1R2 or hT1R3 monomers with Brz resulted in a hT1R2-Brz or hT1R3-Brz heterodimer. Ala19 of Brz interacts with the cytoplasmic helix P828-D839 of hT1R2. In the hT1R3, Brz interacts with two sites in VFTM. In the first binding site, Brz interacts with its Ala19 (Assadi-Porter et al., 2010). Site-directed mutagenesis of Ala19 demonstrated its importance for the sweetness effect of Brz (Ghanavatian et al., 2016). In the second binding site of hT1R3, Brz Tyr54 forms a cation-π bond with Arg536 of hT1R3. The C-terminal residue Tyr54 is has been shown to be important for sweetness (Assadi-Porter et al., 2010). Therefore, these experimental results support the accuracy of AF-M for predicting peptide-protein interactions.

Do Gur-1 and Gur-2 bind to T1R2/T1R3 heterodimers and/or to T1R2 and T1R3 monomers and thus preventing their dimerization? To answer this question, AF-M is used with (Gur-1, T1R2), (Gur-1, T1R3), and (Gur-1, T1R2, T1R3) amino acid sequences. AF-M produces five ranked models. Each of the five predicted structure has been examined. This explains why two binding sites for Gur-1 or Gur-2 were found in some assays. AF-M predicted that Gur-1 and Gur-2 interact with intracellular and extracellular

regions of T1R2/T1R3. Indeed, Gur-1 and Gur-2 bind to the intracellular domain (ICD) of mouse and human T1R2 monomer and to the T1R2 subunit of the T1R2/T1R3 heterodimer (Fig. 5 and 6) with binding affinities of -7.4 to -10.2 kcal/mol (Table 2).

Table 2. Predicted interactions by AF-M of Gur-1, Gur-2, T1R2 and T1R3

Input for AF-M	Binding site	Binding affinity (kcal mol-1)
mT1R2, Gur-1	ICD	-8.1
mT1R3, Gur-1	CRD near VFTM, CRD near TMD	-8.9, -7.3
mT1R2, mT1R3, Gur-1	ICD mT1R2, CRD near TMD mT1R2	-8.4, -7.1
mT1R2, Gur-2	ICD, CRD near TMD	-7.4, -8.9
mT1R3, Gur-2	CRD near TMD	-9.7
mT1R2, mT1R3, Gur-2	ICD mT1R2, CRD near TMD mT1R2	-8.3, -7.7
hT1R2, Gur-1	ICD	-8.8
hT1R3, Gur-1	CRD, CRD near TMD	-7.3, -6.9
hT1R2, hT1R3, Gur-1	ICD hT1R2	-10.2
hT1R2, Gur-2	ICD	-8.9
hT1R3, Gur-2	CRD near TMD, CRD near TMD	-6.4, -6.3
hT1R2, hT1R3, Gur-2	ICD hT1R2, TMD hT1R2	-8.1, -5.6

AF-M : AlphaFold-Multimer.
Mouse T1R2 (mT1R2); human T1R2 (hT1R2)
VFTM : Venus flytrap module; CRD: cysteine rich domain; TMD : trans-membrane domain; ICD : intracellular domain

The amino acids involved in these interactions are mainly Tyr13-14 and Trp28-29 for Gur-1 and Phe14 and Trp28-29 for Gur-2. The hydrophobic amino acids Tyr14 and Trp29 have been involved in the sweet-suppressing properties of Gur-1 (Ota et al., 1998a; Sigoillot et al., 2018). *In silico* competition assays between Gur-1 and Gur-2 for binding T1R2 as a monomer or in a T1R2/T1R3 heterodimer revealed that Gur-1 binds in the ICD of T1R2, whereas Gur-2 occupies the region between the CRD and TMD of T1R2 (Table 3). Notably, Gur-1 binds T1R2 monomer with affinities of -9.4 and -10.4 kcal/mol, whereas in T1R2/T1R3 heterodimer Gur-1 sticks to the ICD of T1R2. This binding of Gur-1 to the ICD may explain the long-lasting suppressive effect of Gur-1 (>2-3 h) (Imoto et al., 1991) and the ineffectiveness of the washing procedures (Sigoillot et al., 2018). Furtheremore, the recovery of Gur-1 suppressive effect is rapid when the tongue of mice was rinsed with β-cyclodextrin (βCD) solution (Murata et al., 2003). This suggests that βCD may enter the cell and remove Gur-1 from the ICD of T1R2 by interacting with Tyr13-14 and Trp28-29 amino acid residues (Imoto et al., 2001). Interestingly, AF-M predicted that Gα-gustducin binds in the same region as Gur-1 and

Gur-2 (see section ‘‘Interaction of T1R2/T1R3 and Gα-gustducin’’ below). This fact may also explain the long-lasting suppressive effect of Gur-1.

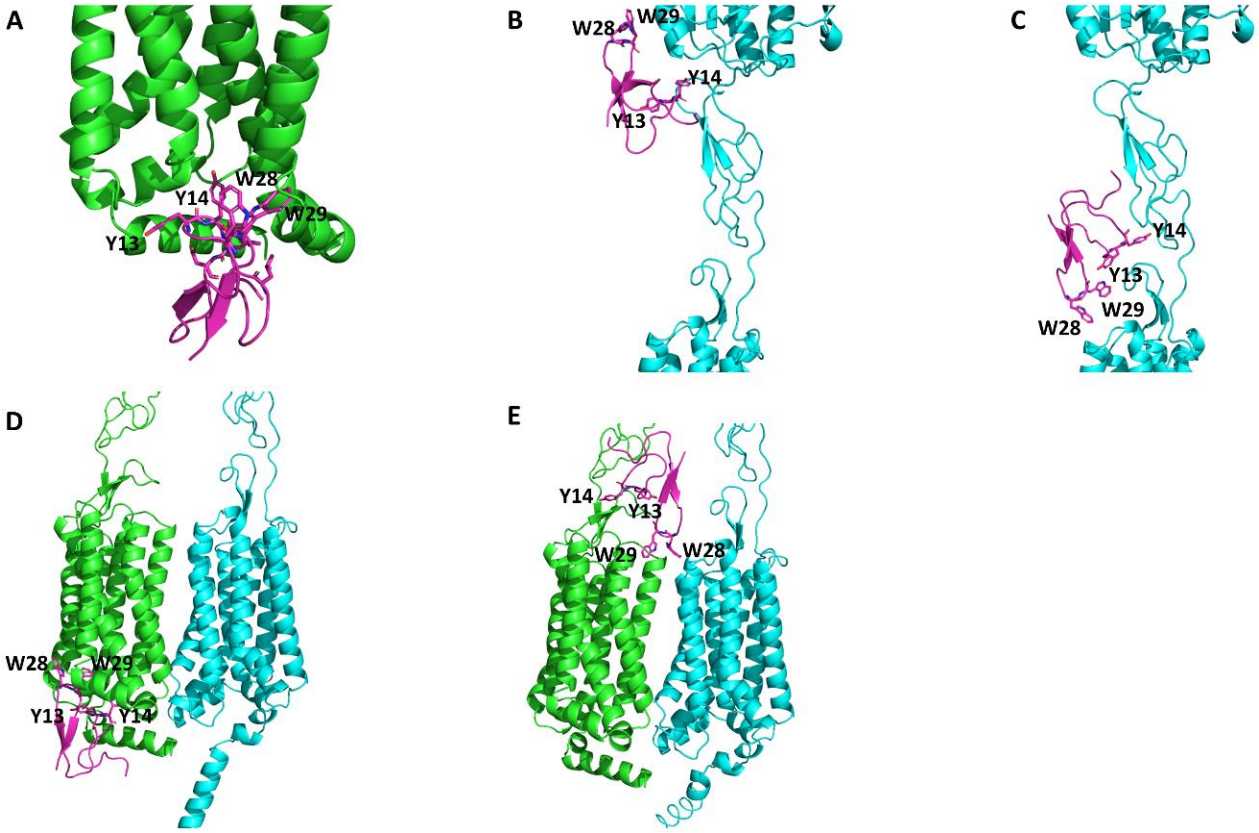

Fig. 5. Interactions of Gur-1 with mouse T1R2, T1R3 monomers and T1R2/T1R3 heterodimer. (**A**) Gur-1 (pink) binds in the intracellular domain (ICD) of T1R2 (green) with Y13, Y14, W28 and W29 amino acid residues. (**B**) and (**C**) Gur-1 binds in cysteine rich domain (CRD) near VFTM and CRD near TMD of T1R3 (cyan), respectively. (**D**) and (**E**) Gur-1 binds in ICD and CRD near TMD of T1R2 subunit of T1R2/T1R3 heterodimer (green/cyan), respectively.

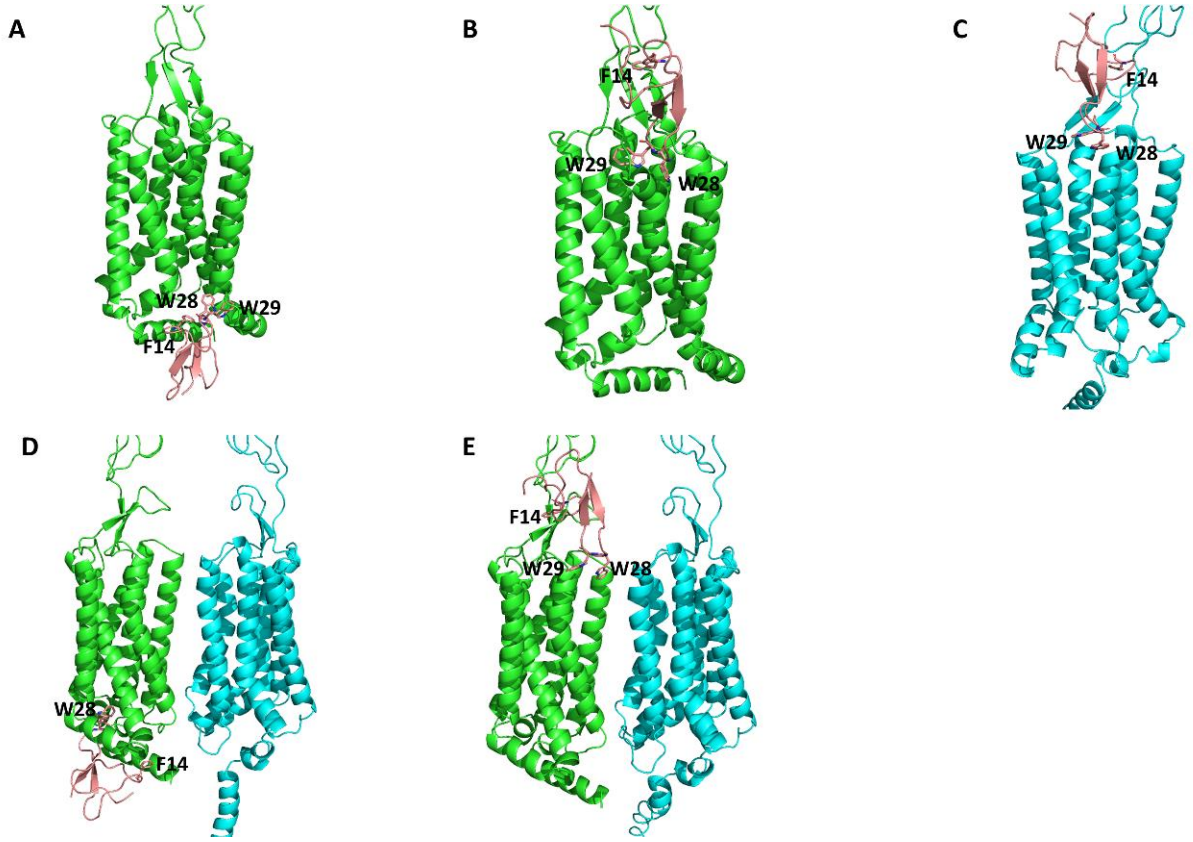

Fig. 6. Interactions of Gur-2 with mouse T1R2, T1R3 monomers and T1R2/T1R3 heterodimer. (**A**) and (**B**) Gur-2 (salmon) binds in the ICD and in CRD near TMD of mT1R2 (green) with F14, W28 and W29 amino acid residues. (**C**) Gur-2 binds in CRD near TMD of mT1R3. (**D**) and (**E**) Gur-2 binds in ICD and CRD near TMD of T1R2 subunit of T1R2/T1R3 heterodimer (green/cyan), respectively.

The use of AF-M with two sequences of mT1R2 and one sequence of Gur-1 or Gur-2 showed only the formation of mT1R2/T1R2 homodimers, but not mT1R2-Gur-1 or mT1R2-Gur-2 heterodimers. The same result was obtained with two sequences of mT1R3 and one sequence of Gur-1 or Gur-2. It has been suggested that the putative homodimerization of T1R3 is not functional (Shimizu et al., 2014). Recently, Belloir and coworkers found that the overexpressed hT1R2 predominantly a dimer (Belloir et al., 2021). Heterodimerization of T1R2 and T1R3 is known to be required for sweet taste perception. This confirms that Gur-1 and Gur-2 interact only with the monomer and heterodimer of T1R2 and T1R3.

Why does Gur-1 suppress sweet taste in rodents but not in humans? The predicted results of interactions of Gur-1 with mouse and human T1R2 and T1R3 are similar. The explanation for the sweet taste suppression by Gur-1 in rodents but not in humans is probably the result of the difference of surface localization of T1R3. In humans T1R3 depends on the co-expression of T1R2. This suggests that hT1R3 and hT1R2 must be in a heterodimeric form for surface localization of a functional sweet taste receptor. In contrast, in mice, T1R3 was expressed without T1R2 expression (Shimizu et al., 2014). It is possible that heterodimerization of mT1R2 and mT1R3 occurs at the cell surface. Therefore, Gur-1 may bind to CRD near FVTM and/or CRD near TMD of mT1R3 monomer (Fig. 5), blocking the formation of the mT1R2/T1R3 heterodimer, and thus suppressing the sweet taste function.

In silico competition assays between Gur-1 and Gur-2

In silico competition assays (Chang and Perez, 2023; Banerjee et al., 2023) between Gur-1 and Gur-2 to bind mT1R3 or hT1R3 give the same results as mT1R3 or hT1R3 with single peptide (Table 3). However, Gur-1 and Gur-2 with mT1R2 or hT1R2 give different results compared to mT1R2 or hT1R2 with single peptide. In fact, an *in silico* competition assay between Gur-1 and Gur-2 to bind hT1R2 showed that only Gur-2 is able to bind the ICD of hT1R2. In the case of mT1R2, Gur-1 binds to the same region (ICD) as in the absence of competition from Gur-2, but Gur-2 binds to VFTM, whereas in the absence of competition from Gur-1 it binds to ICD. Finally, *in silico* competition assays between Gur-1 and Gur-2 to bind both mT1R2 and mT1R3 or their human homologues showed the binding of Gur-1 to the ICD of T1R2 and Gur-2 to the CRD near the TMD of T1R3 (Table 3).

Table 3. *In silico* assay competitions between Gur-1, Gur-2, T1R2 and T1R3

Input for AF-M	Binding site	Binding affinity (kcal mol-1)
mT1R2, Gur-1, Gur-2	ICD Gur-1, CRD near TMD Gur-2	-10.4, -7.8
mT1R3, Gur-1, Gur-2	CRD near VFTM Gur-1, CRD Gur-2	-9.9, -7.6
mT1R2, mT1R3, Gur-1, Gur-2	ICD mT1R2 Gur-1, CRD near TMD mT1R3 Gur-2	N.D, -6.4
hT1R2, Gur-1, Gur-2	ICD Gur-1, CRD near TMD Gur-2	-9.4, -7.2
hT1R3, Gur-1, Gur-2	ICD Gur-1, CRD near TMD Gur-2	-9.6, -6.6
hT1R2, hT1R3, Gur-1, Gur-2	ICD hT1R2 Gur-1, CRD near TMD hT1R3 Gur-2	N.D, -5.7

N.D: not determined

No interactions of Gur-3 to Gur-9 are seen with monomers nor heterodimers of T1R2 and T1R3. This suggests that Gur-3 to Gur-9 may have functions other than interacting with the sweet taste receptor.

To know whether the binding of Gur-1 or Gur-2 to monomers or the complex T1R2/T1R3 changes the conformation of the complex, the pairwise structure alignment of mouse T1R2/T1R3 and T1R2/T1R3-Gur-1 complexes was performed. It showed an RMSD of 2.17 Å at 824 amino acid residues of T1R2-Gur-1 compared to T1R2. For Gur-2, the RMSD is of 1.89 Å on 824 amino acid residues of mT1R2. For human, a RMSD of 1.6 Å on 820 amino acid residues of T1R2 binds Gur-1 relative to T1R2, and 1.76 Å on 818 amino acid residues for Gur-2. These results showed that Gur-1 induces an important conformational change of T1R2 in mouse than in human. And compared to Gur-1, Gur-2 has less effect on the conformation change. These results suggest that Gur-1, especially in the mouse, induces a destabilization of the active conformation of T1R2/T1R3. This, among other factors, may explain why Gur-1 acts as a sweet taste suppressor in rodents but not in humans.

Molecular dynamics simulation

Only Gur-1 and Gur-2 among all gurmarin-like peptides interact with the sweet taste receptor as shown above. They share 51% of identity in amino acids and are structurally aligned with an RMSD of 0.94 Å on all amino acid residues.

Gur-1 and Gur-2 show some differences in binding to the T1R2 and T1R3 monomers. In fact, Gur-1 binds only to the ICD of mT1R2, whereas Gur-2 binds to the ICD and CRD near the TMD of mT1R2 (Table 2). In mT1R3, Gur-1 binds to two regions, CRD near VFTM and CRD near TMD, whereas Gur-2 only interacts with CRD near TMD of mT1R3 (Fig. 5 and 6). To explain this difference, molecular dynamics (MD) simulations with Gur-1 and Gur-2 for 100 ns were conducted in GROMACS to compare their stability and conformational changes. As shown in Fig.7B, Gur-2 has less conformational flexibility than Gur-1. The most flexible part of Gur-1 and Gur-2 is the N-terminal extremity. Interestingly, the two other more flexible regions are those containing Tyr13/Tyr14 and Trp28/Trp29 amino acids of Gur-1. This result is consistent with that of

Sigoillot et al. who demonstrated that a dynamic behavior for the Tyr13–Asp16 amino acid cluster, especially for the Trp28/Trp29 residues. Tyr13/Tyr14 and Trp28/Trp29 are important for the suppressive effect of Gur-1 (Sigoillot et al., 2018), and were found to interact with T1R2 and T1R3 in this study. Of note, the difference in the flexibility between Gur-1 and Gur-2 is more pronounced in the region containing Trp28/Trp29. To characterize the dynamic changes of the whole peptide, the time evolution of the radius of gyration (Rg) and SASA of Gur-1 and Gur-2 are displayed (Fig. 7C and D). Rg and SASA of Gur-2 indicate that its structure is more compact, and its surface is less exposed compared to Gur-1. These results may explain why Gur-1 and Gur-2 interact with different regions of T1R3 and why Gur-2 has a higher affinity for hT1R2 than Gur-1.

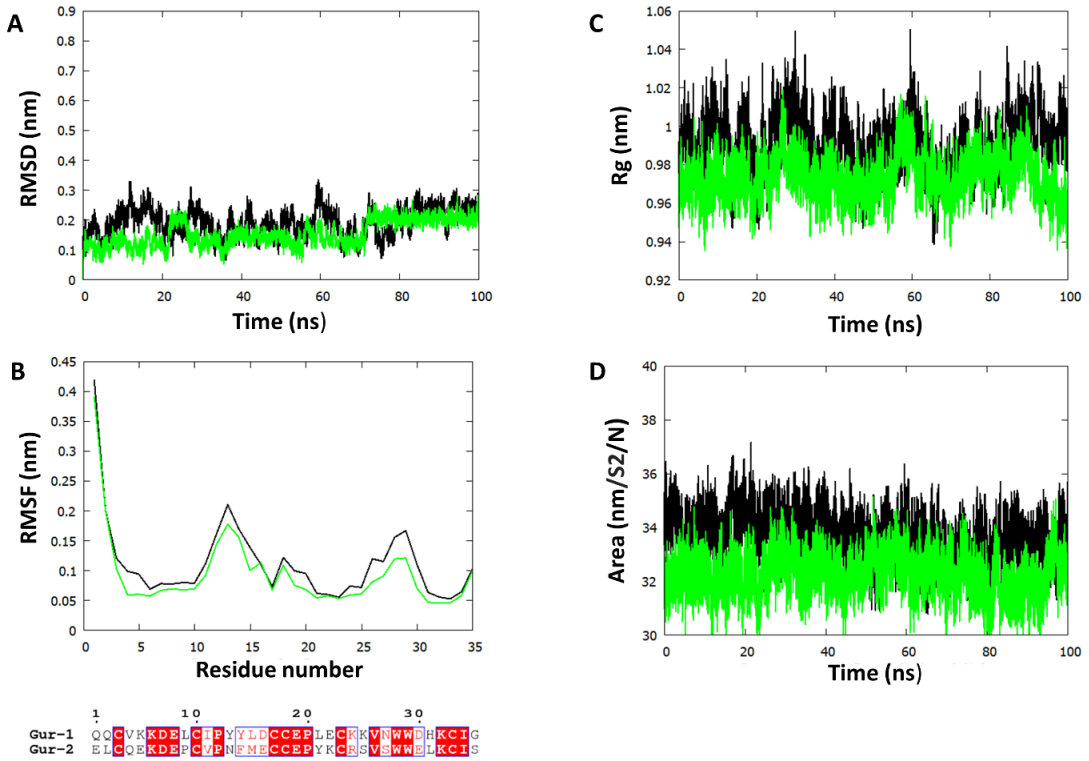

Fig. 7. Molecular dynamics simulations (100 ns) for the peptides Gur-1 (black curve), Gur-2 (green curve). **A**, Time evolution of Root mean square deviation (RMSD) with respect to initial structure. **B**, root mean square fluctuations (RMSF) of peptides residues. The position of amino acid residues in alignment is identical to this in RMSF plot. **C**, radius of gyration (Rg) and solvent-accessible surface area (SASA).

Interaction of T1R2/T1R3 and Gα-gustducin

It is known that T1R2/T1R3 is coupled with Gα-gustducin, and lead to downstream signaling for sweet perception (Lindemann, 2001; Yasumatsu et al., 2009). For Gur-1, Gα-gustducin has been shown to be a key molecule involved in the transduction pathway for Gur-1 sensitive sweet responses (Shigemura et al., 2008; Ohkuri et al., 2009; Yasumatsu et al., 2009).

AF-M predicted that mouse Gα-gustducin (mGα-gustducin) interacts only with the mT1R2 subunit of mT1R2/T1R3 complex. This is in agreement with the results of Sainz and coworkers, who suggested that the T1R2 subunit in sweet taste receptor is responsible for the activation of the coupled G protein (Sainz et al., 2007), and of Liu and coworkers, who showed that heterodimeric metabotropic glutamate receptors (mGlus) transduce signals with one specific subunit that activates G protein (Liu et al., 2017). In addition, the C-terminus Cys351, Leu353 and Phe354 residues of mGα-gustducin interact with Thr820, Ile816 and Met658 residues of the mT1R2 subunit of the mT1R2/T1R3 complex, respectively. This result is consistent with the work of Hara et al. (2012), which showed that the last C-terminus 37 amino acid residues of Gα-gustducin are important for its activity in yeast (Hara et al., 2012). Additionally, a point mutation Gly352Pro of Gα-gustducin impaired its ability to activate taste GPCRs (Ruiz-Avila et al., 2001). It is likely that the Gly352Pro mutation destabilizes the region containing residues Cys351, Leu353 and Phe354, preventing Gα-gustducin to the binding to receptor.

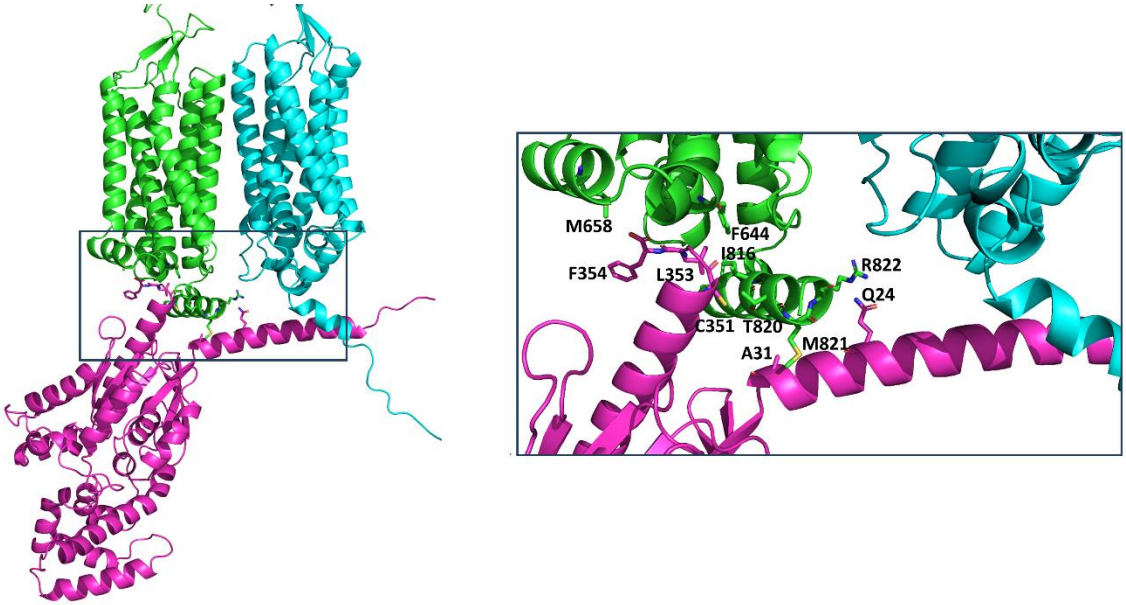

Fig. 8. Interaction of Gα-gustducin with mouse T1R2/T1R3. Gα-gustducin (pink) binds to intracellular domain (ICD) of T1R2 (green) subunit of T1R2/T1R3 heterodimer (green/cyan). Amino acid residues of T1R2 and T1R3 are numbering without signal peptide.

Since mGα-gustducin binds in the same region as Gur-1, it is likely that Gur-1 competes with mGα-gustducin for binding to mT1R2, and may explain the long-lasting suppressive effect (>2-3 hours) of Gur-1.

References

Assadi-Porter, F.M., Maillet, E.L., Radek, J.T., Quijada, J., Markley, J.L., and Max, M. 2010. Key amino acid residues involved in multi-point binding interactions between brazzein, a sweet protein, and the T1R2-T1R3 human sweet receptor. J Mol Biol. 398:584–599.

Ayachit, G., Shaikh, I., Sharma, P., Jani, B., Shukla, L., Sharma, P., Bhairappanavar, S.B., Joshi, C., and Das, J. 2019. De novo transcriptome of Gymnema sylvestre identified putative lncRNA and genes regulating terpenoid biosynthesis pathway. Sci Rep. 9:14876.

Banerjee, S., Varga, J.K., Kumar, M., Zoltsman, G., Isupov, M.N., Rosenzweig, R., Schueler-Furman, O., and Wiener, R. 2023. Structural study of UFL1-UFC1 interaction uncovers the importance of UFL1 N-terminal helix for ufmylation. BioRxiv.

Belloir, C., Brulé, M., Tornier, L., Neiers, F., and Briand, L. 2021. Biophysical and functional characterization of the human TAS1R2 sweet taste receptor overexpressed in a HEK293S inducible cell line. Sci Rep. 11:22238.

Bezençon, C., Coutre, J. le, and Damak, S. 2007. Taste-signaling proteins are coexpressed in solitary intestinal epithelial cells. Chem Senses. 32:41–49.

Chang, L., and Perez, A. 2023. Ranking Peptide Binders by Affinity with AlphaFold**. Angew Chem Int Ed. 62:e202213362.

Cui, M., Jiang, P., Maillet, E., Max, M., Margolskee, R.F., and Osman, R. 2006. The heterodimeric sweet taste receptor has multiple potential ligand binding sites. Curr Pharm Des. 12:4591–4600.

Devangan, S., Varghese, B., Johny, E., Gurram, S., and Adela, R. 2021. The effect of Gymnema sylvestre supplementation on glycemic control in type 2 diabetes patients: A systematic review and meta-analysis. Phytother Res PTR. 35:6802–6812.

Evans, R., O'Neill, M., Pritzel, A., Antropova, N., Senior, A., Green, T., Žídek, A., Bates, R., Blackwell, S., Yim, J., et al. 2022. Protein complex prediction with AlphaFold-Multimer. BioRxiv.

Ghanavatian, P., Khalifeh, K., and Jafarian, V. 2016. Structural features and activity of Brazzein and its mutants upon substitution of a surfaced exposed alanine. Biochimie. 131:20–28.

Guindon, S., Dufayard, J.-F., Lefort, V., Anisimova, M., Hordijk, W., and Gascuel, O. 2010. New algorithms and methods to estimate maximum-likelihood phylogenies: assessing the performance of PhyML 3.0. Syst Biol. 59:307–321.

Gutierrez, S., Tyczynski, W.G., Boomsma, W., Teufel, F., and Winther, O. 2022. MembraneFold: Visualising transmembrane protein structure and topology. 2022.12.06.518085.

Hara, K., Inada, Y., Ono, T., Kuroda, K., Yasuda-Kamatani, Y., Ishiguro, M., Tanaka, T., Misaka, T., Abe, K., and Ueda, M. 2012. Chimeric Yeast G-Protein α Subunit Harboring a 37-Residue C-Terminal Gustducin-Specific Sequence Is Functional in *Saccharomyces cerevisiae*. Biosci Biotechnol Biochem. 76:512–516.

Holm, L. 2020. Using Dali for Protein Structure Comparison. Methods Mol Biol Clifton NJ. 2112:29–42.

Imoto, T., Miyasaka, A., Ishima, R., and Akasaka, K. 1991. A novel peptide isolated from the leaves of Gymnema sylvestre--I. Characterization and its suppressive effect on the neural responses to sweet taste stimuli in the rat. Comp Biochem Physiol A. 100:309–314.

Imoto, T., Sasamoto, K., and Ninomiya, Y. 2001. Beta-cyclodextrin inhibits the sweet taste suppressing activity of gurmarin by the formation of an inclusion complex with aromatic residues in gurmarin. Can J Physiol Pharmacol. 79:836–840.

Jumper, J., Evans, R., Pritzel, A., Green, T., Figurnov, M., Ronneberger, O., Tunyasuvunakool, K., Bates, R., Žídek, A., Potapenko, A., et al. 2021. Highly accurate protein structure prediction with AlphaFold. Nature. 596:583–589.

Kalariya, K.A., Gajbhiye, N., Minipara, D., Meena, R.P., Kumar, S., Saha, A., Trivedi, A., and Manivel, P. 2019. Deep sequencing-based de novo transcriptome analysis reveals biosynthesis of gymnemic acid in Gymnema sylvestre (Retz.) Schult. Ecol Genet Genomics. 13:100047.

Kalariya, K.A., Minipara, D.B., and Manivel, P. 2018. De novo transcriptome analysis deciphered polyoxypregnane glycoside biosynthesis pathway in Gymnema sylvestre. 3 Biotech. 8:381.

Kamei, K., Takano, R., Miyasaka, A., Imoto, T., and Hara, S. 1992. Amino acid sequence of sweet-taste-suppressing peptide (gurmarin) from the leaves of Gymnema sylvestre. J Biochem (Tokyo). 111:109–112.

Kaminski, G.A., Friesner, R.A., Tirado-Rives, J., and Jorgensen, W.L. 2001. Evaluation and Reparametrization of the OPLS-AA Force Field for Proteins via Comparison with Accurate Quantum Chemical Calculations on Peptides. J Phys Chem B. 105:6474–6487.

Katoh, K., and Toh, H. 2008. Recent developments in the MAFFT multiple sequence alignment program. Brief Bioinform. 9:286–298.

Kempen, M. van, Kim, S.S., Tumescheit, C., Mirdita, M., Lee, J., Gilchrist, C.L.M., Söding, J., and Steinegger, M. 2023. Fast and accurate protein structure search with Foldseek. Nat Biotechnol.

Kohno, D., Koike, M., Ninomiya, Y., Kojima, I., Kitamura, T., and Yada, T. 2016. Sweet Taste Receptor Serves to Activate Glucose- and Leptin-Responsive Neurons in the

Hypothalamic Arcuate Nucleus and Participates in Glucose Responsiveness. Front Neurosci. 10:502.

Kyriazis, G.A., Soundarapandian, M.M., and Tyrberg, B. 2012. Sweet taste receptor signaling in beta cells mediates fructose-induced potentiation of glucose-stimulated insulin secretion. Proc Natl Acad Sci U S A. 109:E524-532.

Lin, Z., Akin, H., Rao, R., Hie, B., Zhu, Z., Lu, W., Smetanin, N., Verkuil, R., Kabeli, O., Shmueli, Y., et al. 2023. Evolutionary-scale prediction of atomic-level protein structure with a language model. Science. 379:1123–1130.

Lindemann, B. 2001. Receptors and transduction in taste. Nature. 413:219–225.

Liu, J., Zhang, Z., Moreno-Delgado, D., Dalton, J.A., Rovira, X., Trapero, A., Goudet, C., Llebaria, A., Giraldo, J., Yuan, Q., et al. 2017. Allosteric control of an asymmetric transduction in a G protein-coupled receptor heterodimer. ELife. 6:e26985.

Maaroufi, H., Potvin, M., Cusson, M., and Levesque, R.C. 2021. Novel antimicrobial anionic cecropins from the spruce budworm feature a poly-L-aspartic acid C-terminus. Proteins. 89:1205–1215.

Masuda, K., Koizumi, A., Nakajima, K., Tanaka, T., Abe, K., Misaka, T., and Ishiguro, M. 2012. Characterization of the modes of binding between human sweet taste receptor and low-molecular-weight sweet compounds. PloS One. 7:e35380.

Miyasaka, A., and Imoto, T. 1995. Electrophysiological characterization of the inhibitory effect of a novel peptide gurmarin on the sweet taste response in rats. Brain Res. 676:63–68.

Mosinger, B., Redding, K.M., Parker, M.R., Yevshayeva, V., Yee, K.K., Dyomina, K., Li, Y., and Margolskee, R.F. 2013. Genetic loss or pharmacological blockade of testes-expressed taste genes causes male sterility. Proc Natl Acad Sci U S A. 110:12319–12324.

Murata, Y., Nakashima, K., Yamada, A., Shigemura, N., Sasamoto, K., and Ninomiya, Y. 2003. Gurmarin suppression of licking responses to sweetener-quinine mixtures in C57BL mice. Chem Senses. 28:237–243.

Nakagawa, Y., Nagasawa, M., Yamada, S., Hara, A., Mogami, H., Nikolaev, V.O., Lohse, M.J., Shigemura, N., Ninomiya, Y., and Kojima, I. 2009. Sweet taste receptor expressed in pancreatic beta-cells activates the calcium and cyclic AMP signaling systems and stimulates insulin secretion. PloS One. 4:e5106.

Nelson, G., Hoon, M.A., Chandrashekar, J., Zhang, Y., Ryba, N.J., and Zuker, C.S. 2001. Mammalian sweet taste receptors. Cell. 106:381–390.

Ninomiya, Y., and Imoto, T. 1995. Gurmarin inhibition of sweet taste responses in mice. Am J Physiol. 268:R1019-1025.

Ohkuri, T., Yasumatsu, K., Horio, N., Jyotaki, M., Margolskee, R.F., and Ninomiya, Y. 2009. Multiple sweet receptors and transduction pathways revealed in knockout mice by temperature dependence and gurmarin sensitivity. Am J Physiol Regul Integr Comp Physiol. 296:R960-971.

Ota, M., Shimizu, Y., Tonosaki, K., and Ariyoshi, Y. 1998a. Role of hydrophobic amino acids in gurmarin, a sweetness-suppressing polypeptide. Biopolymers. 45:231–238.

Ota, M., Shimizu, Y., Tonosaki, K., and Ariyoshi, Y. 1998b. Synthesis, characterization, and sweetness-suppressing activities of gurmarin analogues missing one disulfide bond. Biopolymers. 46:65–73.

Ozden, B., Kryshtafovych, A., and Karaca, E. 2023. The Impact of AI-Based Modeling on the Accuracy of Protein Assembly Prediction: Insights from CASP15. Bioinformatics.

Pallaghy, P.K., Nielsen, K.J., Craik, D.J., and Norton, R.S. 1994. A common structural motif incorporating a cystine knot and a triple-stranded beta-sheet in toxic and inhibitory polypeptides. Protein Sci Publ Protein Soc. 3:1833–1839.

Park, J., Selvam, B., Sanematsu, K., Shigemura, N., Shukla, D., and Procko, E. 2019. Structural architecture of a dimeric class C GPCR based on co-trafficking of sweet taste receptor subunits. J Biol Chem. 294:4759–4774.

Ren, X., Zhou, L., Terwilliger, R., Newton, S.S., and Araujo, I.E. de. 2009. Sweet taste signaling functions as a hypothalamic glucose sensor. Front Integr Neurosci. 3:12.

Ruiz-Avila, L., Wong, G.T., Damak, S., and Margolskee, R.F. 2001. Dominant loss of responsiveness to sweet and bitter compounds caused by a single mutation in alpha -gustducin. Proc Natl Acad Sci U S A. 98:8868–8873.

Sainz, E., Cavenagh, M.M., LopezJimenez, N.D., Gutierrez, J.C., Battey, J.F., Northup, J.K., and Sullivan, S.L. 2007. The G-protein coupling properties of the human sweet and amino acid taste receptors. Dev Neurobiol. 67:948–959.

Shigemura, N., Nakao, K., Yasuo, T., Murata, Y., Yasumatsu, K., Nakashima, A., Katsukawa, H., Sako, N., and Ninomiya, Y. 2008. Gurmarin sensitivity of sweet taste responses is associated with co-expression patterns of T1r2, T1r3, and gustducin. Biochem Biophys Res Commun. 367:356–363.

Shimizu, M., Goto, M., Kawai, T., Yamashita, A., and Kusakabe, Y. 2014. Distinct human and mouse membrane trafficking systems for sweet taste receptors T1r2 and T1r3. PloS One. 9:e100425.

Sigoillot, M., Brockhoff, A., Lescop, E., Poirier, N., Meyerhof, W., and Briand, L. 2012. Optimization of the production of gurmarin, a sweet-taste-suppressing protein, secreted by the methylotrophic yeast Pichia pastoris. Appl Microbiol Biotechnol. 96:1253–1263.

Sigoillot, M., Brockhoff, A., Neiers, F., Poirier, N., Belloir, C., Legrand, P., Charron, C., Roblin, P., Meyerhof, W., and Briand, L. 2018. The Crystal Structure of Gurmarin, a Sweet Taste-Suppressing Protein: Identification of the Amino Acid Residues Essential for Inhibition. Chem Senses. 43:635–643.

Teufel, F., Refsgaard, J.C., Kasimova, M.A., Deibler, K., Madsen, C.T., Stahlhut, C., Grønborg, M., Winther, O., and Madsen, D. 2023. Deorphanizing Peptides Using Structure Prediction. J Chem Inf Model. 63:2651–2655.

Xue, L.C., Rodrigues, J.P., Kastritis, P.L., Bonvin, A.M., and Vangone, A. 2016. PRODIGY: a web server for predicting the binding affinity of protein-protein complexes. Bioinforma Oxf Engl. 32:3676–3678.

Yasumatsu, K., Ohkuri, T., Sanematsu, K., Shigemura, N., Katsukawa, H., Sako, N., and Ninomiya, Y. 2009. Genetically-increased taste cell population with G(alpha)-gustducin-coupled sweet receptors is associated with increase of gurmarin-sensitive taste nerve fibers in mice. BMC Neurosci. 10:152.

Yoshie, S., Miyasaka, A., and Imoto, T. 1994. Histological localization of the sweet taste receptor in rat taste buds by the use of gurmarin, a sweet taste-suppressing peptide. Arch Histol Cytol. 57:531–534.

Supplementary Material

Table 1S. Structural alignment of Gur-2 to Gur-9 with Gur-1

	Z-score	RMSD (A)	Length alignment	Residues number	% Identity
Gur-1	8.8	0.0	35	35	100
Gur-2	7.2	0.9	35	35	51
Gur-3	6.0	1.4	34	34	35
Gur-8	5.1	2.1	35	43	31
Gur-6	5.0	2.0	33	36	42
Gur-9	5.0	2.1	34	36	32
Gur-4	5.0	2.0	33	33	24
Gur-5	4.4	2.8	34	35	21
Gur-7	3.9	2.3	33	37	30

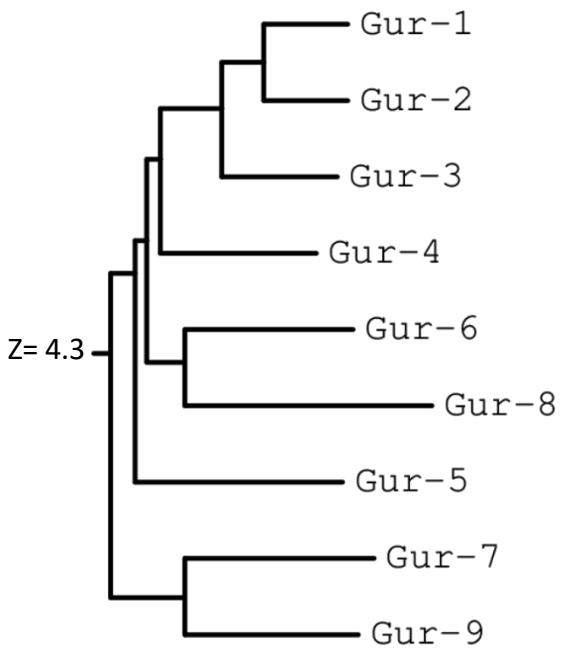

Fig. 1S. Structural similarity dendrogram of Gur-1 to Gur-9. Labels are linked to structural summaries. The dendrogram is derived by average linkage clustering of the structural similarity matrix (Dali Z-scores, see table 1S above).